JOURNAL OF THE ROYAL SOCIETY Interface

J. R. Soc. Interface (2012) **9**, 727–733
doi:10.1098/rsif.2011.0424
Published online 24 August 2011

Staining diatoms with rhodamine dyes: control of emission colour in photonic biocomposites

Melanie Kucki† and Thomas Fuhrmann-Lieker*

Department of Mathematics and Science, Institute of Chemistry and Center for Interdisciplinary Nanostructure Science and Technology, Kassel University, Heinrich-Plett-Strasse 40, 34109 Kassel, Germany

The incorporation of rhodamine dyes in the cell wall of diatoms *Coscinodiscus granii* and *Coscinodiscus wailesii* for the production of luminescent hybrid nanostructures is investigated. By systematic variation of the substitution pattern of the rhodamine core, we found that carbonic acids are considerably better suited than esters because of their physiological compatibility. The amino substitution pattern that controls the optical properties of the chromophore has no critical influence on dye uptake and incorporation, thus a variety of biocomposites with different emission maxima can be prepared. Applications in biomineralization studies as well as in materials science are envisioned.

Keywords: biological photonic crystals; biomineralization; fluorescence

1. INTRODUCTION

Diatoms (Bacillariophyta) have been fascinating the scientific community owing to their intricate cell wall with pores arranged in various patterns—up to highly ordered periodic structures in the micrometre- and submicrometre range for some species. As biochemical investigations show, the material consists not only of hydrated silica but also has an organic component of polyamines and silaffine proteins, the composition of which strongly depends on the species that is considered [1,2]. Recently, even the presence of ultraviolet light-absorbing mycosporine-like amino acids was detected [3].

The mesoscopic architecture of the cell wall (frustule) attracted much interest in materials science and nanotechnology [4]. Recent examples include in addition to the classical application in filter technology, specific surface functionalization [5] and transformation of the structure into other material systems by templating techniques [6]. Optical properties of the cell wall, their biological function and possible applications have been discussed [7,8]. We demonstrated that the cell wall can be regarded from an optical point of view as a photonic crystal slab wave guide since in the thin wave guiding layer, a regular periodic pattern of high and low effective refractive index is defined by the pore array [9]. Such photonic crystals generally exhibit optical resonances at certain frequencies that can be used for wave coupling or stimulated emission. In species of the genus *Coscinodiscus*, different patterns with distinct optical properties can be found (figure 1): the valve exhibits a hexagonal pore array with micrometre periodicity, whereas the girdle is characterized by a square pattern of 250–300 nm periodicity that has resonances in the optical frequency range [9]. The extent to which this general property of being a 'biological photonic crystal' has an influence on the diatom photobiology is an open speculation. Interestingly, the chloroplasts especially of the species with the most regular arrays (order Centrales) are located directly next to the cell wall; thus, wave guiding effects may play a role.

In order to address the question of photonic properties of the cell wall, tools are needed to measure light confinement effects within the cell wall for a broad spectral range. For this task, fluorescent dyes are a possible solution. In addition to the covalent attachment of dyes at isolated cell walls via silicon chemistry, we apply the method of *in vivo* fluorochromation with laser dyes as probe molecules for the optical modes [10]. Such fluorescent markers have been used for monitoring biomineralization processes by staining the siliceous cell wall. Dyes that have been reported as suitable for that purpose are Rhodamine 123 [11], the oxazole dye PDMPO (or LysoSensor Yellow/Blue DND-160, Invitrogen) [12], the benzoxadiazole dye HCK-123 [13] and two oxadiazole dyes [14].

This report contains a systematic study on the application of rhodamine laser dyes with the twofold aim of increasing the palette of dyes adaptable for certain spectral ranges and establishing a structure–property relationship between the chemical substitution pattern of the rhodamine core and the accumulation of the dyes in the cell wall. All investigated dyes are capable of stimulated emission in solution because of their high fluorescence quantum yield with low reabsorption; thus, they are highly suitable for the investigation of photonic confinement effects.

*Author for correspondence (th.fuhrmann@uni-kassel.de).
†Present address: INM Leibniz Institute for New Materials, Nano Cell Interactions, Campus D2 2, 66123 Saarbruecken, Germany.

Electronic supplementary material is available at http://dx.doi.org/10.1098/rsif.2011.0424 or via http://rsif.royalsocietypublishing.org.

Received 1 July 2011
Accepted 1 August 2011

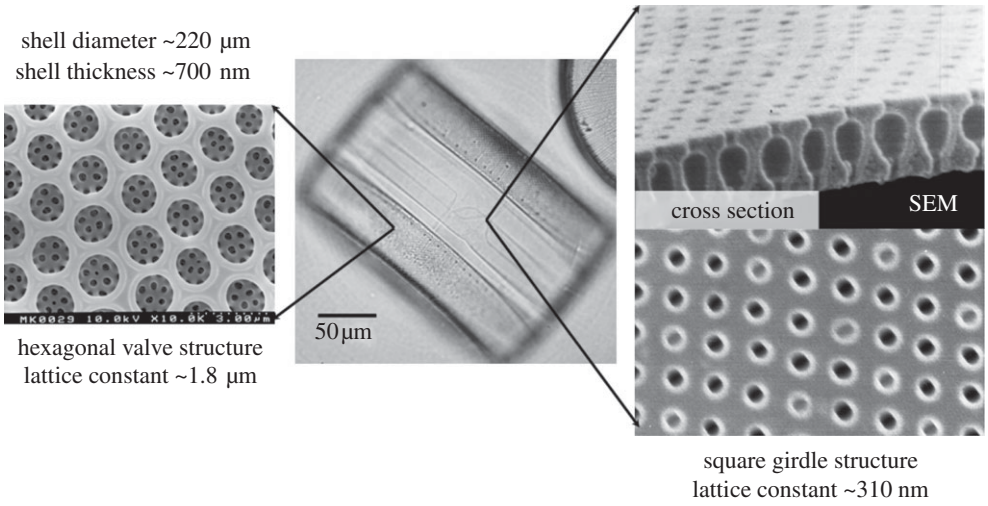

Figure 1. Cell wall morphology of *Coscinodiscus wailesii* with valve and girdle patterns. Central image taken by optical microscopy and details by scanning electron microscopy.

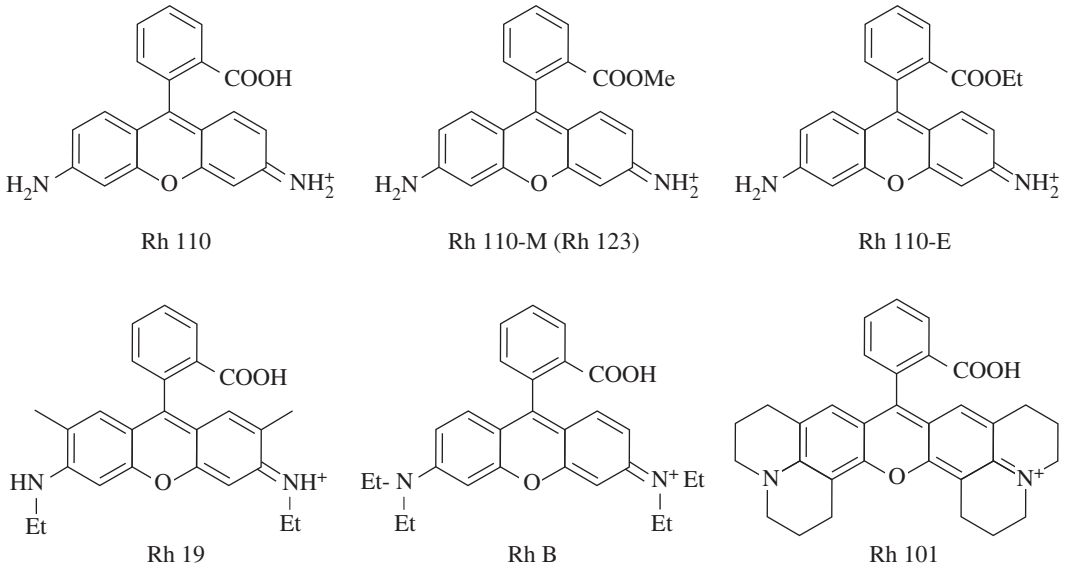

Figure 2. Chemical structures of rhodamine dyes.

2. EXPERIMENTAL

The diatom species *Coscinodiscus granii* and *Coscinodiscus wailesii* were cultivated in semi-artificial sea water medium in batch culture. Both cultures were derived from strains maintained at the University of Regensburg collected from the North Sea (Germany). Details of the cultivation conditions can be found in the electronic supplementary material. Unless otherwise stated, staining was performed by the addition of a 10 mM solution of the dye in dimethylsulphoxide (DMSO; p.a. $\geq$99.5%) to the culture medium in order to obtain a concentration of 1 µM.

Twelve rhodamine (Rh) dyes with systematically varied substitution patterns were investigated. The rhodamine core is characterized by two main functionalities: the 3,6-diamino substituents at the xanthene moiety and the 2-carboxy function at the phenyl ring. In order to investigate the influence of the amine, a primary amine (Rh 110), a secondary amine (Rh 19), a tertiary amine (Rh B) and an amine with julolidine bridging (Rh 101) was chosen (figure 2). In order to investigate the influence of the carboxy function, the free carboxylic acids were compared with the corresponding methyl esters (denoted as Rh 110-M, Rh 19-M, Rh B-M, Rh 101-M) and ethyl esters (Rh 110-E, Rh 19-E, Rh B-E, Rh 101-E). Rh 110-M is a synonym of the above-mentioned Rh 123, and Rh 19-E is commonly known as the widely applied laser dye Rhodamine 6G. The synthesis of the methyl and ethyl esters from the corresponding acid compounds follows the procedure given by Ramos *et al.* [15]. A comprehensive table of the investigated dyes can be found in the electronic supplementary material.

Stained frustules were treated with hot 0.1 M Na–EDTA–2 per cent sodium dodecylsulphate solution in order to remove the majority of the organic components of the cell wall. Fluorescence spectra were recorded with a Hitachi F-4500 fluorescence spectrophotometer.

Table 1. Absorption and fluorescence maxima of investigated dyes in dimethylsulphoxide (DMSO) solution, and emission maxima from stained frustules. Unsuccessful incorporation owing to death of the cells is indicated. M, methyl ester derivative; E, ethyl ester derivative.

	abs. (DMSO; nm)	emission (DMSO; nm)	cell status after incubation*	emission (frustule; nm)
Rh 110	518	539	vital	535
Rh 110-M (Rh 123)	519	545	vital	544
Rh 110-E	519	548	dead	—
Rh 19	535	561	vital	546
Rh 19-M	539	565	dead	—
Rh 19-E (Rh 6G)	539	564	dead	—
Rh B	564	592	vital	573
Rh B-M	566	593	dead	—
Rh B-E	566	593	dead	—
Rh 101	580	606	vital	581, 622
Rh 101-M	588	615	dead	—
Rh 101-E	588	615	dead	—

*At a standard concentration of 1 μM dye and an incubation time of 3 days or longer.

Microscopic images were taken with an Olympus IX70+IX-FLA epifluorescence microscope equipped with a mercury lamp as the light source and U-MWU2, U-MNB2 and U-MNG2 filter modules for ultraviolet, blue and green excitation, respectively. The microscope was connected to an Ocean Optics S2000 fibre-optics spectrometer that allowed the recording of spatially resolved local emission spectra.

Confocal laser scanning microscope images were recorded using a Leica TCS SP system with excitation at 488 and 543 nm. Prior to microscopical investigation of living cells, the cells were rinsed with fresh sea water medium to minimize the fluorescence background.

Scanning electron microscopy investigations were performed using a Hitachi S-4000 system at an accelerating voltage of 10 kV after coating the samples with platinum.

3. RESULTS AND DISCUSSION

To investigate the possibility of producing a functional biocomposite material containing laser dyes as one of its constituents, an exposure time of several hours to days is needed. Although in most *in vivo*-fluorochromation procedures, exposure to dyes is usually restricted to several minutes, we followed the uptake for many generations in non-synchronized cultures. In this sense, fluorochromation with a dye is said to be successful if the cells do not receive significant physiological damage that prevents cell division even during prolonged exposure, and if the dye was incorporated into both thecae (the halves of the Petri-dish-like shaped cell wall), which demonstrates successful incorporation over at least two generations as in every division step a new hypotheca (lower half) is formed. Depending on the growth conditions, exposure times of several hours to days were applied. The maximum exposure time tested in this work was eight weeks, after which the cultures were still capable of reproduction.

3.1. Variation of the amino function in rhodamine stains

All rhodamines used are water-soluble, chemically stable and exhibit low photobleaching rates and high quantum yields [16]. The absorption and fluorescence behaviour of a rhodamine are primarily dependent on the size and character of the amino substituents at the xanthene core. The higher the alkylation of the amino groups the less is the influence of solvent polarity and temperature on the fluorescence of the rhodamine. A rigidization of the dye molecule by incorporation of the julolidine ring structure leads to a further decrease in rotational activation of the excited dye molecules and increases the fluorescence quantum yield. The quantum yield of Rh 101 in solution is virtually 100 per cent, independent on temperature. The additional alkyl substitution at the xanthene chromophore of Rh 19 and Rh 101 has no influence on the spectroscopic properties [16]. Absorption and emission maxima of the dyes are given in table 1. In the following, only the dyes with free carboxylic groups (Rh 110, Rh 19, Rh B, Rh 101) are discussed, whereas the esters will be discussed in §3.2.

Microscopical analysis of the diatom cells showed that incubation with the above-mentioned rhodamine dyes does not lead to visible morphological alterations of the cell frustules. Incubation led to fluorescent cell wall structures within 1–3 days (figure 3). Dense cell wall structures that consist of a high amount of silica per area showed a more intense fluorescence when compared to structures with lower silica content per area. No morphological aberrations of the cell wall structures were observable. Even after incubation time of eight weeks, as tested in the case of Rh 110, cells were vital and capable of division, leading to fluorescent cell walls. If *in vivo*-fluorochromated cells were washed in dye-free medium (twice for 5–10 min, until the cells were sedimented), then most of the fluorescence of the inner part of the cell was lost. Some structures retain the rhodamine dyes longer than others, but a very tight bonding of the dye exists only at the cell walls. After isolation of the cell walls from the living cell, they still showed a bright fluorescence.

For the two *Coscinodiscus* species investigated, all four rhodamine dyes (Rh 110, Rh 19, Rh B, Rh 101) were incorporated successfully. Rh B has been tested as a stain before, but contradictory results on the

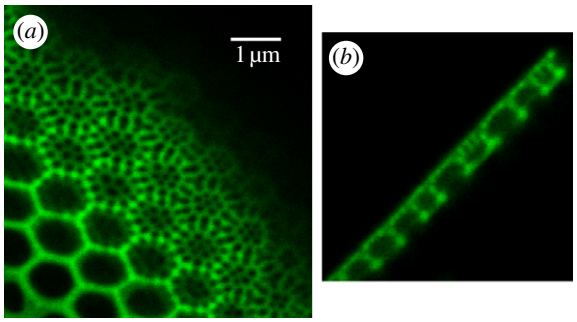

Figure 3. Details of successfully stained cell walls taken by confocal laser scanning microscopy. (*a*) Optical cut through the valve of *Coscinodiscus wailesii* stained with Rh 19. (*b*) Cross section of the valve of *C. wailesii* stained with Rh 19. (Online version in colour.)

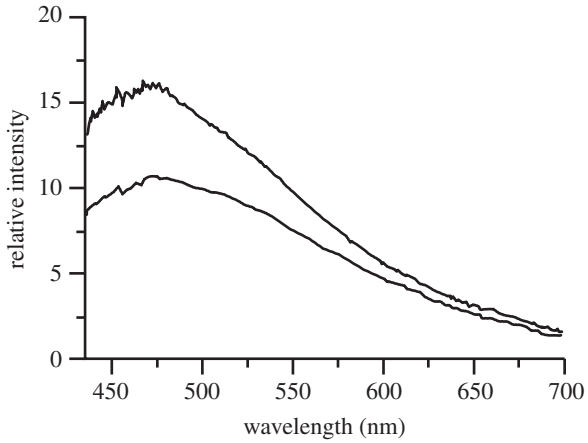

Figure 4. Autofluorescence of an unstained frustule of *Coscinodiscus granii*. The lower spectrum is taken 2 min after the upper spectrum, indicating photobleaching under UV irradiation (excitation at 330–385 nm).

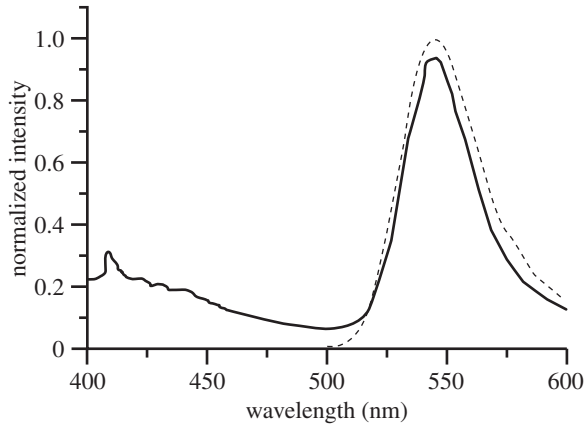

Figure 5. Fluorescence spectrum of living diatom cells (*Coscinodiscus wailesii* fluorochromated with Rh 19, rinsed and free of unbound dye) at two irradiation wavelengths (solid line: 325 nm, dotted line: 480 nm). The autofluorescence below 500 nm resulting from various components of the intact cell represents an upper limit for cell wall autofluorescence.

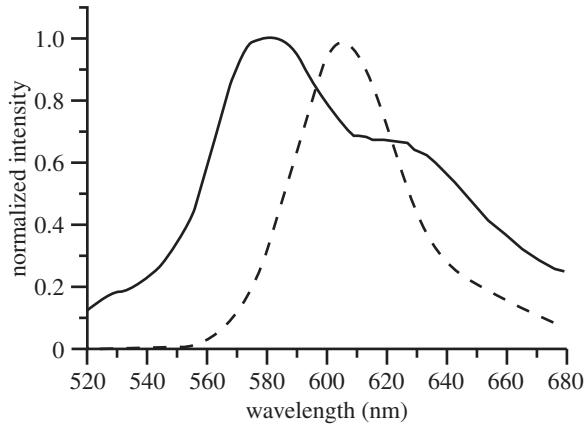

Figure 6. Fluorescence spectrum of Rh 101 in dilute dimethylsulphoxide solution (dotted line) and in the isolated valve of *Coscinodiscus granii* in air (solid line).

incorporation into plant cells are reported. Höfler [17] reported on harmful effects on *Biddulphia*, whereas Weber found no damage in the higher plant *Helodea* [18]. We found that in the case of *Coscinodiscus*, the cells remained vital, as with the three other stains.

Emission spectra were taken from living cells after removal of excess dye by rinsing as well as from isolated frustules. As reference background, the fluorescence emission of unstained frustules was measured. A weak but clearly detectable broad autofluorescence emission band with maximum at 470 nm in the case of *C. granii* (figure 4) was measured. Interestingly, visible fluorescence was reported for diatoms before, but in some cases with other spectral characteristics [19–23]. The origin of this fluorescence is not clear but can in principle either arise from the organic matrix that may contain heterocyclic moieties [3] or from surface states in mesoporous silica [24,25].

The emission of stained frustules is much more pronounced and is characterized by structure-less emission bands in the green to red spectral regions (figure 5). After isolation and purification of the frustules, this emission remained. Autofluorescence is still visible, but with lower intensity, and can be seen as background in the spectra. Rh 110 exhibits a maximum at 535 nm in water which is red-shifted with respect to the emission spectrum of the unbound dye in water (522 nm) and blue-shifted with respect to the dye in DMSO (539 nm). A shift may be explained by solvent polarity or acid–base equilibria. Based on the fact that protonation of the carboxylic group generally does not lead to a band shift larger than about 3 nm [16,26], we conclude that the shift indicates a change of polarity in the microenvironment of the dye with respect to aqueous solution.

Similarly, the emission of Rh 19 in living cells of *C. granii* (546 nm) and *C. wailesii* (545 nm) is not as bathochromically shifted as in DMSO solution. In air, the fluorescence maximum of isolated frustules is 537 nm. Rh B emits yellow, with a maximum of 573 nm in living as well as in isolated cells. Finally, the emission of Rh 101 is in the orange–red spectral region, with a maximum of 580 nm and as additional feature a pronounced shoulder at 622 nm (figure 6). In this case, the local environment clearly influences the chromophore, as only one peak at 606 nm can be detected in DMSO solution. Interestingly, the same

spectral characteristics with two emission bands can also be detected in the fluorochromation of other species such as testate amoebae for which the technique described for diatoms worked as well. Summarizing this section, rhodamines of different amino substitution patterns can be used for fluorochromation, leading to emitting diatom frustules in a wide spectral range.

3.2. Variation of the carboxylic group in rhodamine stains

The carboxyl substituent of the phenyl group has a minor influence on the location of absorption and emission bands. It is not part of the chromophore, but it locks the phenyl ring into an orthogonal position, thus decreasing rotational deactivation of excited dye molecules and increasing the quantum yield [16]. Systematic variation of the group by esterification with methanol and ethanol was performed in order to elucidate the influence of this group on the incorporation.

For comparison, tests were performed for both diatom species with the standard stain concentration of 1 µM, and all samples were cultured in parallel with a reference sample free of any dye supplementation. In strong contrast to the samples with free carboxylic groups, all esters with one exception resulted in morphological alterations of the cell: alteration of the chloroplast distribution and chloroplast shape as well as detachment and shrinkage of the cytoplasm. The notable exception is the methyl ester Rh 110-M alias Rh 123 that has been previously applied as a biomineralization marker in diatoms. All other esters proved to be toxic and finally lethal within several hours to a few days, irrespective of the counter ion used for stabilizing the protonated form (chloride or perchlorate). For Rh 19-E (Rh 6G), these findings are congruent with studies on higher plant species and fungal cells [18,27,28] but are in contrast to experiments of Hildebrand & Palenik [29] on the pennate diatom *Navicula pelliculosa*.

In the staining experiments, the dyes clearly accumulated in cell compartments around the nucleus, presumably mitochondria. At several points, the cytoplasm started to detach from the cell wall and to draw back to the centre of the cell. The chloroplast changes from lobed to round as a sign of the alteration of cell physiology and forthcoming cell death [30].

For the interpretation of the different behaviour of carboxylic acids and their corresponding esters, the molecular charge may play an important role. It is known that rhodamines with a net positive charge selectively stain mitochondria, whereas rhodamines that are net uncharged at physiological pH show no specific staining owing to the highly negative potential difference across the mitochondrial membrane [31,32]. A prolonged stay of the rhodamine molecules inside the mitochondria can lead to inhibition of vital cell growth. This might be owing to a disturbance of the oxidative phosphorylation. A cleavage of the ester bond may occur in order to release methanol or ethanol. For zwitterionic dyes such as the carboxylic acids, the low pH of the silica deposition vesicles may change the equilibrium distribution of the dyes between the distinct cellular compartments and thus account for the preferred accumulation into the cell wall without disturbing the cell physiology.

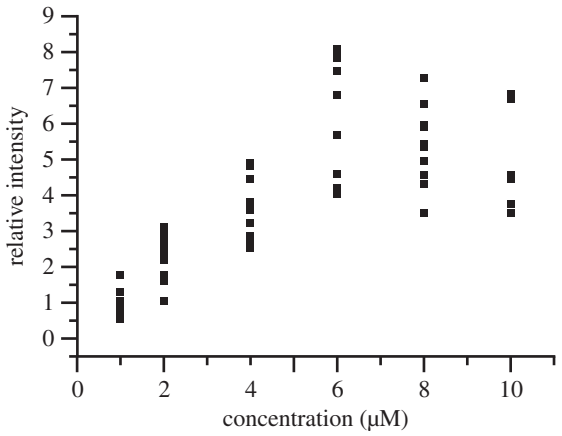

Figure 7. Relative peak emission intensity of cells cultured in the presence of different concentrations of Rh 19 and rinsed in fresh medium.

Another effect that may contribute to the distinct behaviour are differences in phototoxicity. Gaboury [33] investigated rhodamines for their application in photodynamic therapy and reported phototoxicity for rhodamine B *n*-butyl ester on cell viability of K562 (chronic myelogenous leukaemia) cells, whereas Rh 123 showed no significant phototoxic effects. A dye structurally related to Rh 101 but without carbonic acid function, chloromethyl-X-rosamine, leads to apoptosis in human osteosarcoma cells as a result of phototoxicity [34]. Thus, phototoxicity has to be taken into account when using rhodamine dyes, but our results show that unsubstituted carboxylic acids can be applied safely for staining, at least with moderate light intensities.

In conclusion of this section, suitable staining dyes for the cell wall of diatoms are the rhodamines with free carboxylic acids and not their ester derivatives because of the cytotoxicity of the latter which prevents large-scale production of fluorescent frustules.

3.3. Dose-dependent fluorescence

With the aim of producing fluorescent composite nanostructures, the maximum amount of dye accumulation is interesting. In addition, toxicity is of course also a function of dose of exposition. In order to address this question, staining tests on *C. wailesii* were performed with different Rh 19 concentrations from 1 to 10 µM in the culture medium. At rhodamine concentrations up to 6 µM, the average peak emission intensity of comparable samples after removing excess dye scaled roughly proportional with the dye concentration. Instead of a saturation behaviour indicating maximum deposition rates, the fluorescence decreased again at concentrations larger than 6 µM (figure 7). Even at the maximum applied concentration of 10 µM and an exposure time of several days (20 days), the majority of the cells were of normal appearance (figure 8, see figure caption for details about chloroplast morphology).

Thus, fluorescence emission can be optimized by choosing an appropriate moderate concentration of

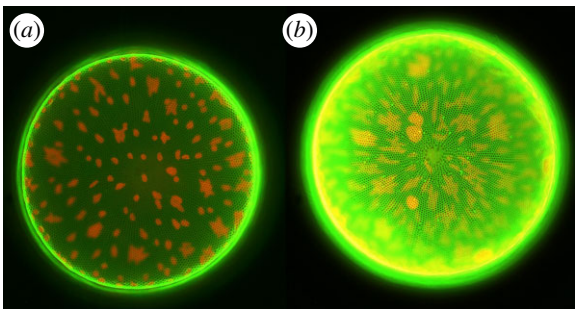

Figure 8. Comparison of the fluorescence of living diatom cells (*Coscinodiscus wailesii*) cultivated in Rh 19 concentration of (*a*) 1 μM and (*b*) 10 μM. Pictures taken with identical microscope and dual-channel camera settings. Besides the fluorescence of the stained frustule, the autofluorescence of the chloroplasts can be seen. Morphological changes of the chloroplasts are caused by the prolonged exposure to intense light during the experiment (cf. [30]). Valve diameter is approximately 220 μM. (Online version in colour.)

the fluorochromation stain. Limitations in the dye deposition and concentration quenching effects of fluorescence may play a role in the nonlinear relationship between fluorescence intensity and concentration.

4. CONCLUSION

We systematically investigated the incorporation of rhodamine dyes in diatom cell walls as 'light-emitting biological photonic crystals' and the correlation with chemical structure. Using the free acids and not the esters is the key to obtain vital self-reproducing structures. By different substitution of the amino groups, the conjugated chromophore can be changed, leading to fluorescent molecules within a wide spectral range from green to red. With these tools, the influence of the optical nanostructure on dyes can be addressed for diatoms under natural and artificial conditions (e.g. photosynthesis and stimulated emission) in further work.

We are indebted to Prof. M. Sumper, Regensburg, for helpful discussions and starting cultures. We also thank Prof. M. Maniak and H. Rühling, Kassel, for experimental support with confocal laser scanning microscopy and scanning electron microscopy, respectively, and Dr Stefan Richter, Halle, for the opportunity of performing spectroscopic control experiments. The support of Dr Manfred Kussler in rhodamine ester synthesis is gratefully acknowledged. Part of this work was funded by the Deutsche Forschungsgemeinschaft under contract No. Fu 450/1 within the priority programme 1113 photonic crystals, and by a PhD Scholarship for Women in Engineering and Natural Sciences, University of Kassel.

REFERENCES

1 Kröger, N., Deutzmann, R. & Sumper, M. 1999 Polycationic peptides from diatom biosilica that direct silica nanosphere formation. *Science* **286**, 1129–1132. (doi:10.1126/science.286.5442.1129)
2 Sumper, M. & Brunner, E. 2006 Learning from diatoms: nature's tool for the production of nanostructured silica. *Adv. Funct. Mater.* **16**, 17–27. (doi:10.1002/adfm.200500616)
3 Ingalls, A. E., Whitehead, K. & Bridoux, M. C. 2010 Tinted windows: the presence of the UV absorbing compounds called mycosporine-like amino acids embedded in the frustules of marine diatoms. *Geochim. Cosmochim. Acta* **74**, 104–115. (doi:10.1016/j.gca.2009.09.012)
4 Parkinson, J. & Gordon, R. 1999 Beyond micromachining: the potential of diatoms. *Tibtech* **17**, 190–196. (doi:10.1016/S0167-7799(99)01321-9)
5 Rosi, N. L., Thaxton, C. S. & Mirkin, C. 2004 Control of nanoparticle assembly by using DNA-modified diatom templates. *Angew. Chem. Int. Ed.* **43**, 5500–5503. (doi:10.1002/anie.200460905)
6 Sandhage, K. H., Dickerson, M. B., Huseman, P. M., Caranna, M. A., Clifton, J. D., Bull, T. A., Heibel, T. J., Overton, W. R. & Schoenwaelder, M. E. A. 2002 Novel, bioclastic route to self-assembled, 3D, chemically tailored meso/nanostructures. *Adv. Mater.* **14**, 429–433. (doi:10.1002/1521-4095(20020318)14:6<429::AID-ADMA429>3.0.CO;2-C)
7 De Stefano, L., Rea, I., Rendina, I., De Stefano, M. & Moretti, L. 2007 Lensless light focussing with the centric marine diatom *Coscinodiscus wailesii*. *Opt. Express* **15**, 18 082–18 088. (doi:10.1364/OE.15.018082)
8 De Tommasi, E., Rea, I., Mocella, V., Moretti, L., De Stefano, M., Rendina, I. & De Stefano, L. 2010 Multi-wavelength study of light transmitted through a single marine diatom. *Opt. Express* **18**, 12 203–12 212. (doi:10.1364/OE.18.012203)
9 Fuhrmann, T., Landwehr, S., El Rharbi-Kucki, M. & Sumper, M. 2004 Diatoms as living photonic crystals. *Appl. Phys. B* **78**, 257–260. (doi:10.1007/s00340-004-1419-4)
10 Kucki, M., Landwehr, S., Rühling, H., Maniak, M. & Fuhrmann-Lieker, T. 2006 Light-emitting biological photonic crystals: the bioengineering of metamaterials. *Proc. SPIE* **6182**, S161 821–S161 829.
11 Li, C.-W., Chu, S. & Lee, M. 1989 Characterizing the silica deposition vesicle of diatoms. *Protoplasma* **151**, 158–163. (doi:10.1007/BF01403453)
12 Shimidzu, K., Del Amo, Y., Brzezinski, M. A., Stucky, G. D. & Morse, D. E. 2001 A novel fluorescent silica tracer for biological silification studies. *Chem. Biol.* **8**, 1051–1060. (doi:10.1016/S1074-5521(01)00072-2)
13 Descles, J., Vartanian, M., El Harrak, A., Quinet, M., Bremond, N., Sapriel, G., Bibette, J. & Lopez, P. J. 2008 New tools for labelling silica in living diatoms. *New Phytol.* **177**, 822–829. (doi:10.1111/j.1469-8137.2007.02303.x)
14 Annenkov, V. V., Danilovtseva, E. N., Zelinskiy, S. N., Basharina, T. N., Safonova, T. A., Korneva, E. S., Likhoshway, Y. V. & Grachev, M. A. 2010 Novel fluorescent dyes based on oligopropylamines for the *in vivo* staining of eukaryotic unicellular algae. *Anal. Biochem.* **407**, 44–51. (doi:10.1016/j.ab.2010.07.032)
15 Ramos, S. S., Vilhena, A. F., Santos, L. & Almeida, P. 2000 ^{1}H and ^{13}C NMR spectra of commercial rhodamine ester derivatives. *Magn. Res. Chem.* **38**, 475–478. (doi:10.1002/1097-458X(200006)38:6<475::AID-MRC662>3.0.CO;2-X)
16 Drexhage, K. H. 1990 Structure and properties of laser dyes. In *Dye lasers* (ed. F. P. Schäfer), pp. 155–200. Berlin, Germany: Springer.
17 Höfler, K. 1963 Zellstudien an *Biddulphia titiana* Grunow. *Protoplasma* **56**, 1–53. (doi:10.1007/BF01249197)
18 Weber, F. 1937 Assimilationsfaehigkeit und Doppelbrechung der Chloroplasten. *Protoplasma* **27**, 460–461. (doi:10.1007/BF01599411)
19 Butcher, K. S. A., Ferris, J. M., Phillips, M. R., Wintrebert-Fouquet, M., Jong Wah, J. W., Jovanovic, N.,

Vyvermann, W. & Chepurnov, V. A. 2005 A luminescence study of porous diatoms. *Mater. Sci. Eng.* **C25**, 658–663.
20 De Stefano, L., Rendina, I., De Stefano, M., Bismuto, A. & Maddalena, P. 2005 Marine diatoms as optical chemical sensors. *Appl. Phys. Lett.* **87**, 233902. (doi:10.1063/1.2140087)
21 Mazumder, N., Gogoi, A., Kalita, R. D., Ahmed, G. A., Buragohain, A. K. & Choudhury, A. 2010 Luminescence studies of fresh water diatom frustules. *Indian J. Phys.* **84**, 665–669. (doi:10.1007/s12648-010-0068-1)
22 Orellana, M. V., Petersen, T. W. & van den Engh, G. 2004 UV-excited blue autofluorescence of *Pseudo-Nitzschia multiseries* (Bacillariophyceae). *J. Phycol.* **40**, 705–710. (doi:10.1111/j.1529-8817.2004.03226.x)
23 Qin, T., Gutu, T., Jiao, J., Chang, C.-H. & Rorrer, G. L. 2008 Photoluminescence of silica nanostructures from bioreactor culture of marine diatom *Nitzschia frustulum*. *J. Nanosci. Nanotechnol.* **8**, 2392–2398. (doi:10.1166/jnn.2008.241)
24 Chiodini, N., Meinardi, F., Morazzoni, F., Paleari, A., Scotti, R. & Di Matrino, D. 2000 Ultraviolet photoluminescence of porous silica. *Appl. Phys. Lett.* **76**, 3209–3211. (doi:10.1063/1.126631)
25 Shieh, J., Cho, A., Lai, Y., Dai, B., Pan, F. & Chao, K. 2004 Stable blue luminescence from mesoporous silica films. *Electrochem. Solid State Lett.* **7**, G319–G322. (doi:10.1149/1.1813251)
26 Ramette, R. W. & Sandell, E. B. 1956 Rhodamine B equilibria. *J. Am. Chem. Soc.* **78**, 4872–4878. (doi:10.1021/ja01600a017)
27 Johannes, H. 1941 Beitraege zur Vitalfaerbung von Pilzmyzelien II. Die Inturbanz der Faerbungen mit Rhodaminen. *Protoplasma* **36**, 181–194. (doi:10.1007/BF01600881)
28 Strugger, S. 1938 Die Vitalfaerbung des Protoplasmas mit Rhodamin B und Rhodamin 6G. *Protoplasma* **30**, 85–100. (doi:10.1007/BF01613719)
29 Hildebrand, M. & Palenik, B. 2003 Investigation into the optical properties of nanostructured silica from diatoms. *Storming Media*. Pentagon report no. A266314M 1–7.
30 Peteler, K. 1939 Amoeboide Formveraenderungen der Diatomeen-Plastiden. *Protoplasma* **32**, 9–19. (doi:10.1007/BF01796940)
31 Johnson, L. V., Walsh, M. L., Bockus, B. J. & Chen, L. B. 1981 Monitoring of relative mitochondrial membrane potential in living cells by fluorescence microscopy. *J. Cell Biol.* **88**, 526–535. (doi:10.1083/jcb.88.3.526)
32 Darzynkiewicz, Z., Traganos, F., Staiano-Coico, L., Kapuscinski, J. & Melamed, M. R. 1982 Interactions of Rhodamine 123 with living cells studied by flow cytometry. *Cancer Res.* **42**, 799–806.
33 Gaboury, L. 1998 Rhodamine derivatives for photodynamic therapy of cancer and in vitro purging of the leukemias. US Patent Publication no. US 5773460 published on 30 June 1998.
34 Minamikawa, T., Sriratana, A., Williams, D. A., Bowser, D. N., Hill, J. S. & Nagley, P. 1999 Chloromethyl-X-rosamine (MitoTracker red) photosensitises mitochondria and induces apoptosis in intact human cells. *J. Cell Sci.* **112**, 2419–2430.